PERGAMON

Journal of Structural Geology 22 (2000) 391–400

JOURNAL OF STRUCTURAL GEOLOGY

www.elsevier.nl/locate/jstrugeo

A new technique to automatically quantify microstructures of fine grained carbonate mylonites: two-step etching combined with SEM imaging and image analysis

Marco Herwegh

Geologisches Institut, Universität Bern, Baltzerstr. 1, 3012 Bern, Switzerland

Received 17 May 1999; accepted 27 October 1999

Abstract

A two-step etching technique for fine-grained calcite mylonites using 0.37% hydrochloric and 0.1% acetic acid produces a topographic relief which reflects the grain boundary geometry. With this technique, calcite grain boundaries become more intensely dissolved than their grain interiors but second phase minerals like dolomite, quartz, feldspars, apatite, hematite and pyrite are not affected by the acid and therefore form topographic peaks. Based on digital backscatter electron images and element distribution maps acquired on a scanning electron microscope, the geometry of calcite and the second phase minerals can be automatically quantified using image analysis software. For research on fine-grained carbonate rocks (e.g. dolomite calcite mixtures), this low-cost approach is an attractive alternative to the generation of manual grain boundary maps based on photographs from ultra-thin sections or orientation contrast images.

1. Introduction

Microfabrics of calcite mylonites contain important information about the condition and kinematics of deformation (e.g. Dietrich and Song, 1984; Burkhard, 1990; Van Der Pluijm, 1991; Burkhard, 1993). Numerous deformation experiments have been performed in the past decades to gain a better understanding about how microfabrics evolve in calcite aggregates under different physical conditions (e.g. Schmid et al., 1977, 1980, 1987; Walker et al., 1990; Casey et al., 1998; Rutter, 1998). As a result, comparison between microstructures of natural and experimental mylonites has become increasingly successful in the interpretation of long lasting deformation histories (e.g. Pfiffner, 1982; Dunlap et al., 1997). Therefore, the quantification of microfabric parameters for both experimentally and naturally deformed rocks and rock analogue materials becomes more and more important (e.g. Pauli et al., 1996; Herwegh and Handy, 1998). While, in the past, optical thin sections have been used to draw grain boundary outlines manually, more recently, new techniques for automatic grain boundary detection (e.g. 'lazy grain boundary' based on a NIH image macro of Heilbronner, 2000) on the optical as well as on the scanning electron microscope have been designed (e.g. Adams et al., 1993; Trimby and Prior, 1999). 'Lazy grain boundary', however, can only be applied to monophase materials of moderate (> several μm) to large grain size, whereas orientation imaging microscopy (i.e. automated EBSD mapping) of Adams et al. (1993) is a time- and cost-intensive approach. Following chemical and thermal etching techniques commonly applied in material sciences, we have designed an additional method using inexpensive two-step etching by acidic liquids to visualise the grain boundaries of extremely fine-grained carbonate mylonites. Although

E-mail address: herwegh@geo.unibe.ch (M. Herwegh).

0191-8141/00/$ - see front matter
PII: S0191-8141(99)00165-0

chemical etching has already been used to visualise grain boundaries (for calcite see e.g. Burkhard, 1990; Walker et al., 1990) and defect structures (see e.g. Wegner and Christie, 1983 and references therein), it has only rarely been combined with automatic grain boundary detection techniques in the earth sciences.

The first part of this article presents: (a) the steps required for surface etching of calcite grains, (b) the computer assisted segmentation of grain boundaries and (c) the combination of grain boundary maps with phase distribution maps producing an image to calculate microstructural parameters. In the second part of the paper the method is used to analyse variations in calcite grain size of a carbonate mylonite in response to changing calcite dolomite volume proportions.

2. Part I: two-step etching

2.1. Technique

The experimental procedure presented in this paper comprises three major steps: (a) sample preparation, (b) image acquisition on the SEM and (c) image analysis.

(a) The principal goal was to find an etching that renders grain boundaries visible so that they

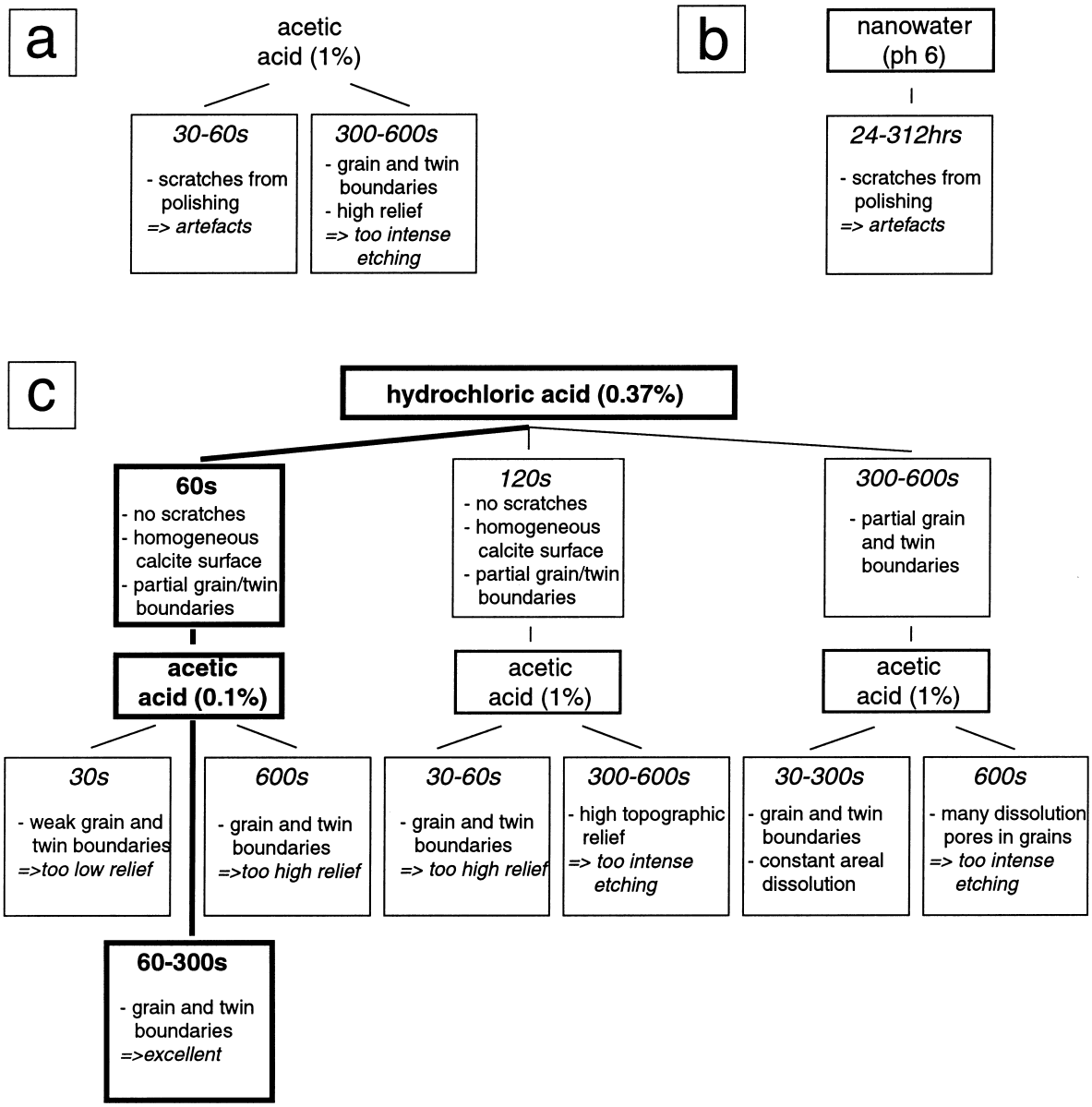

Fig. 1. Flow charts of different etching series with a brief summary of the major results. Best etching sequence is outlined bold.

can be discriminated automatically from the grain interior with digital image analysis techniques. Fine-grained carbonate mylonites (circular equivalent radii 2–40 μm) from the Helvetic nappe stack (Switzerland) were selected for the different etching tests. Most of the calcite grains had straight grain boundaries and only few grains were twinned. The samples were cut into ordinary rock chips with dimensions of $4 \times 2 \times 1\ cm^3$ and glued onto glass slides as used for ordinary thin sections. Grinding with corundum powder (150, 300, 400, 600, 800) and polishing on a DP-Pan polishing disk resulted in a flat polished sample surface.

For the etching procedures 25 ml beakers were filled with 15 ml acidic liquid. Because of the buffering capacity of the acids it is of great importance to keep both rock-chip dimensions and volume proportion of the acid constant. Note that the use of bigger glasses and larger quantities of acid leads to excess etching of the rock chip surfaces.

Hydrochloric acid, acetic acid and nanowater (18 MΩ water) with a pH of about 6 served as etching liquids. Three general etching series were performed using (a) concentrated acids, (b) weak acids and (c) a multistage etching procedure with weak acids (see flow chart in Fig. 1). The etching times varied from 10 to 600 s and 24 to 312 h for the acids and the nanowater, respectively. The concentrations of hydrochloric and acetic acids ranged from 0.37 to 10% and from 0.1 to 10%, respectively.

(b) After etching, the samples were coated with carbon (> 30 nm) and observed in a CamScan (CS4) scanning electron microscope (SEM) equipped with a Voyager 4 system and a Pioneer light element detector (EDS, electron dispersive spectrometer) from Noran. Because of the three-dimensional topography of the etched surfaces, secondary electrons (SE) and backscatter electrons (BSE) were used to generate digital images reflecting topographic contrasts (for more details see Goldstein et al., 1992). Note that the material contrast as shown by BSE (i.e. atomic number contrast) is weakened by the surface relief. For segmentation of the different minerals by image analysis techniques additional element distribution maps were captured using image sizes of 512×512 pixels and acquisition times of 4.5 h.

(c) NIH image 1.61 (http://rsb.info.nih.gov/nih-image/) was used to segment both grain boundary outlines and elemental maps. The combination of phase distribution maps and grain/phase boundary outlines allowed the reconstruction of the microfabric of the carbonate mylonite (see below). Calcite grain orientations and the orientation of the different mineral aggregates were analysed with the computer program PAROR (Panozzo, 1983).

2.2. Etching results

The results of the etching series are summarised in the flow chart of Fig. 1. A procedure with hydrochloric acid (0.37%) and acetic acid (0.1%) and etching times of 60 s and 300 s, respectively, proved to be most successful. The first etching step with hydrochloric acid homogeneously dissolves the calcite surface and destroys high dislocation arrays, which were induced during the polishing procedure in the uppermost surface layer. At the same time, less soluble second phase minerals like dolomite, quartz, hematite and apatite remain as topographic peaks on the surface of the sample. Continued calcite dissolution using acetic acids etches out the grain and twin boundaries in the second step. In many cases grain boundaries are more intensely dissolved than twin boundaries resulting in deeper valleys with stronger contrast. Note that by starting the etching procedure directly with 0.1% acetic acid, one would primarily etch the artificially induced defect structures and therefore highlight an artificially induced field of scratches (Fig. 1).

As a consequence of cutting and polishing the sample, the grains of the aggregate become dissected at different points along their diameter (i.e. tomato salad problem see Exner, 1972; Heilbronner and Bruhn, 1998). In some cases only a small fraction of a grain remains in the block while the counterpart is either cut or polished away. These small end pieces can escape during the etching procedure because they lose their cohesion. As a consequence a hole is left in the surface of the sample which appears as a dark patch in the digital image (see 2 in Fig. 2). Such artefacts must be considered when segmenting the grain boundaries with image analysis software in a later step.

2.3. Image processing

2.3.1. Grain boundary maps of calcite grains

The surface of the carbonate rock attacked by the aforementioned etching procedure is used as a base for the automatic detection of calcite grain boundaries. Based on BSE images (acceleration voltage: 15–20 keV), Fig. 2 shows the steps required to process the digital SEM image in order to obtain a grain boundary map:

1. Contrast is enhanced and noise is reduced by applying the appropriate filters (e.g. contrast, smoothing, median filters) of the image analysis program NIH

image 1.61 (Fig. 2b).

2. The grain boundaries are segmented manually by using the density slice function and the image is saved as a binary file. The principal goal of manually setting the threshold value is to select as much of the dark grain-boundary area as possible without selecting the grey values of the grain interiors (Fig. 2c).
3. Iterative growth and shrinkage cycles by opening and closing procedures are used to improve the connectivity between individual grain boundary segments. This step is similar to the lazy grain boundary method of Heilbronner (2000), but with respect to the quality of the grain boundary map, no more than five iterative steps are recommended.
4. The skeletonize function of NIH image reduces the grain boundary outlines to a constant thickness of one pixel. These lines, however, are too thin for the analysis and have to be thickened by copying and pasting the grain boundary outline both one position to the left and one to the top of the existing image. Using lazy grain boundary (Heilbronner, 2000) facilitates this procedure.
5. Even on well-etched surfaces, grain boundary outlines are not always perfect, i.e. some grain boundaries are not closed, small grain relicts have disappeared or twin boundaries appear as grain boundaries (Fig. 1c). Examples of such artefacts are shown as points 1 and 2 in Fig. 2. In order to produce a high quality grain boundary map, these artefacts must be eliminated manually. This is best done by creating a three layer image (BSE, SE and grain boundary outline) in the program Adobe PhotoShop©. The grain boundaries are corrected on the grain boundary outline layer (opacity 20–40%) using the pen and eraser tools while BSE and SE images serve as originals on the two underlying layers.
6. When a satisfying grain boundary map is obtained, the digital binary image of the grain boundary outlines is inverted (Fig. 2f).
7. Using NIH image 1.61—grain area, grain perimeter, the length of grain major and minor axis as well as the orientation of the long axis of each individual grain is determined. Particles touching the edge of the image are excluded by setting the appropriate

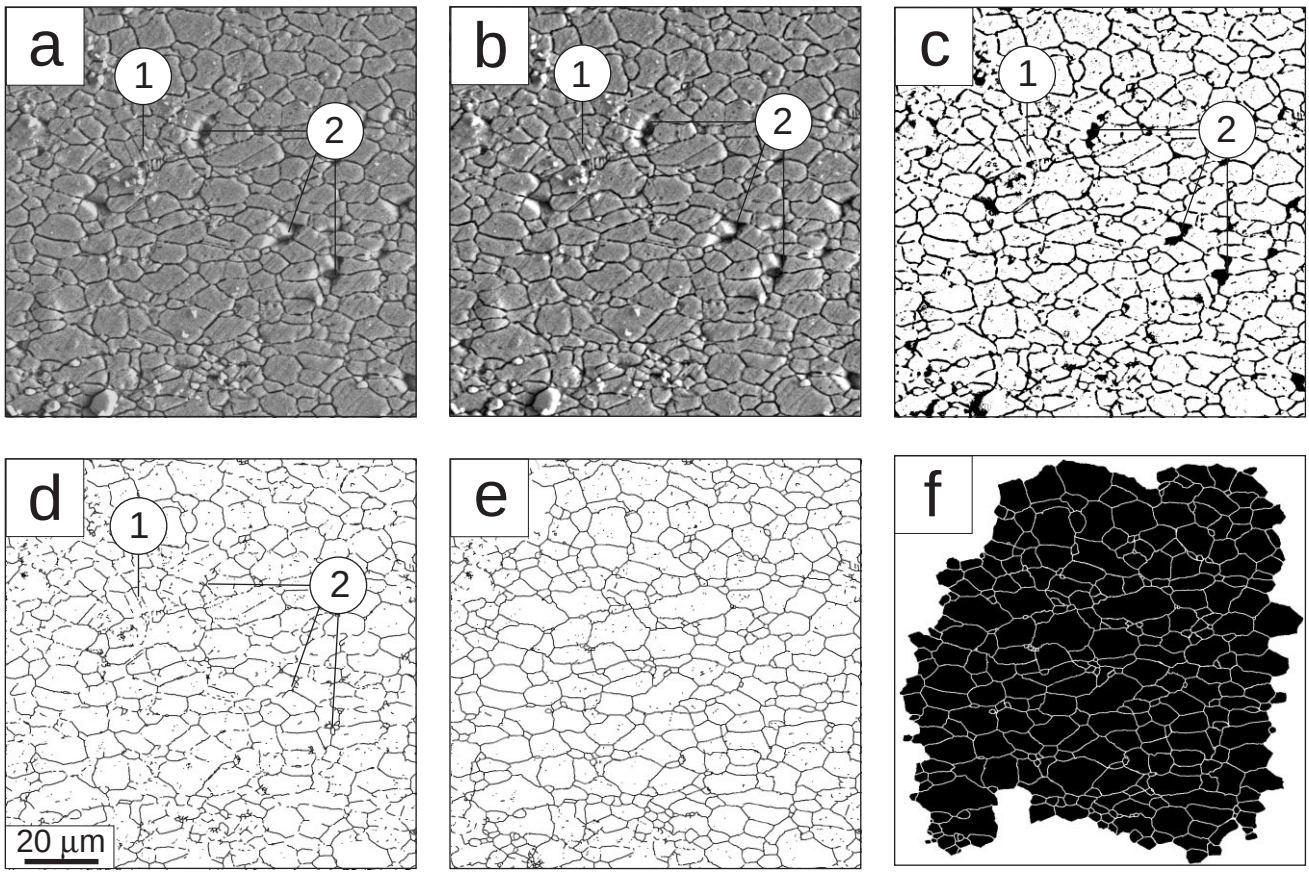

Fig. 2. Steps required to generate a grain boundary outline of the calcite microstructure. (a) Original BSE image, (b) BSE image after smooth/median filtering and enhancing contrast/brightness, (c) segmentation of the grain boundaries and transformation of the grey scale image into a binary image, (d) skeletonization of the grain boundaries, (e) manual improvement of the image and (f) final grain boundary outline. (1) Twin boundaries and (2) surface holes and the resulting artefacts during skeletonization (see text for explanations).

option. Using SURFOR and PAROR (Panozzo, 1983, 1984) the preferred orientations of grains and grain boundary surfaces can be calculated (see for example Fig. 3).

Note that steps 1–4 can also be carried out using the t–j–i subroutines of lazy grain boundary, a macro (NIH image) designed for grain size analysis from optical photomicrographs (Heilbronner, 2000). In contrast to lazy grain boundary, which should only be used for grain size estimations, the two-step etching approach is also designed to obtain grain boundary maps so that particle and surface orientations may also be determined with a high accuracy. Careful completion of step 5 is therefore of great importance.

In order to test the quality of our grain boundary segmentation procedure, two rock chips from the same sample were analysed with the etching technique and with manually derived grain boundary outlines, based on an orientation contrast image (see Prior et al., 1996). The orientation contrast image was acquired from a steeply tilted surface on a CamScan CS LB 44 at the ETH Zurich equipped with forescatter electron detectors (FSE, e.g. Prior et al., 1996). Fig. 3 shows the microstructures and the calculated microstructural parameters (i.e. grain size distribution, ratio of minor/major grain axis, and the orientation of the grain major axis). The microstructure in Fig. 3(a) contains a big calcite grain while more uniform grain sizes occur in Fig. 3(b). This microstructural heterogeneity seems to be responsible for the minor derivations with respect to the grain size interval (Fig. 3c and d) and the orientations of the grain major axes (Fig. 3e and f). Furthermore, the grain boundaries in the orientation contrast image (Fig. 3b) are more regular. This fact might have been artificially induced by the required stretching of this image parallel to the vertical axis (see below). Besides these minor differences the quality of the two techniques with respect to a visualisation of the calcite microstructure is equivalent. Under the assumption that we can exclude similar artefacts for both techniques, etching proves to be a valuable technique to visualise grain boundaries in fine-grained calcite aggregates.

2.3.2. Mineral distribution maps

This approach is very interesting for fine-grained polymineralic carbonates like dolomite–calcite mixtures. As a consequence of the three dimensional relief induced by surface etching, topographic contrast predominates in BSE images and atomic number contrast of different mineral phases is weaker than would be

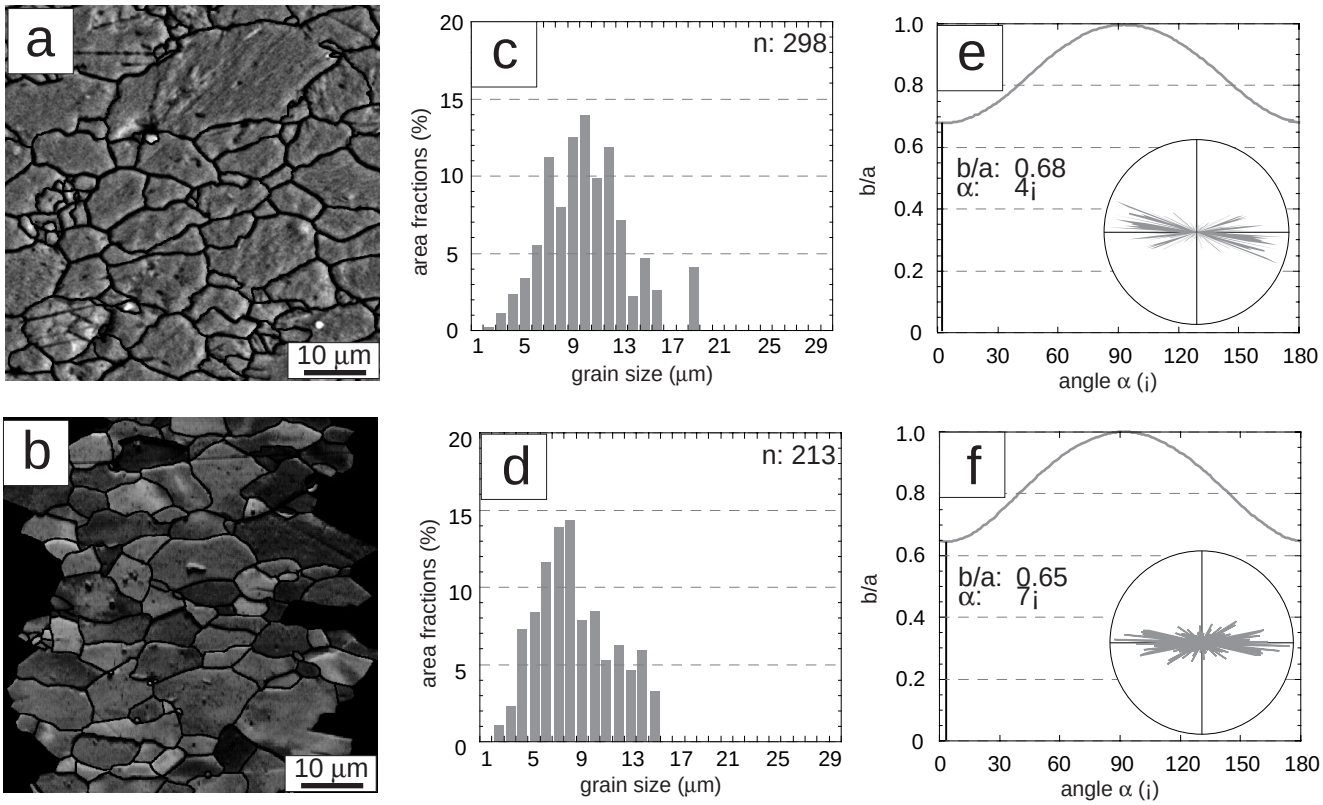

Fig. 3. Microstructure analysis based on an etched calcite surface (upper row) and on an orientation contrast image (lower row). (a and b) Parts of the analysed microstructure, (c and d) grain size vs. grain area fractions, (e and f) ratio minor/major grain axis vs. the angle (α) between the grain's long axis and horizontal. Rose diagrams in insets of (e) and (f) show the orientation of the grain long axes.

the case for flat surfaces. Therefore weak contrasts can become a problem during image segmentation of the different minerals. However, asperities of the surface relief are still small enough to permit acquisition of element distribution maps. Table 1 lists the selected SEM parameters. In order to detect all possible second phase minerals, a mapping strategy must be devised which discriminates the abundant phases using a minimum number of element maps. For calcite mylonites the following elements were mapped: calcium (calcite, dolomite), magnesium (dolomite), silicon (quartz, feldspars), potassium (micas, clay minerals, K-feldspar), phosphorous (apatite), iron (hematite, pyrite) and sulphur (pyrite). Some of the elements occur in more than one phase (e.g. calcium occurs in both dolomite and calcite) but the characteristic X-ray photon count is, as a first approximation, proportional to the element concentration. Along with the occurrence of mineral specific elements (e.g. phosphorous in apatite), this allows the separation of different minerals by grey level thresholding and/or image subtraction. An oxygen map was also acquired at the same time because this light element is extremely sensitive to physical parameters like mineral composition and sample topography induced by the etching. The oxygen map allows visualisation of calcite grain boundaries and distribution of calcite and dolomite phases. The chemical information and microstructural grain boundary outlines of calcite can then be combined into one single digital image allowing further quantification of phase proportions, distributions and spatial orientations with image analysis techniques like NIH image 1.61, SURFOR (Panozzo, 1984), PAROR (Panozzo, 1983) and the auto-correlation function (Panozzo Heilbronner, 1992). In comparison to monomineralic calcite aggregates, the number of artefacts induced by the etching technique is higher. In order to generate accurate grain-boundary outlines of the calcite grains, therefore, more manual corrections are required for the polyphase carbonates.

2.4. Advantages of the two-phase etching approach

Due to the nature of fine-grained carbonate mylonites (0.5–50 μm) with a small number of twinned grains and subgrains, the presented approach is a very inexpensive and suitable method for the characterisation of microstructures. Towards larger grain sizes, however, the number of artefacts (more twin and subgrain boundaries) increases and the contrast quality between grain boundary and interior decreases, so that the two-step etching method becomes less efficient.

Table 1
Selected parameters for elemental mapping on the SEM

acceleration voltage	20 keV
beam current	3.5×10^{-9} A
counts per second	2200
live time	4 h
total time	5 h
image size	512 × 512 pixel

In comparison to manual grain boundary tracings based on images from ultra thin sections the presented method has major advantages: (1) The very difficult and time consuming preparation of ultra thin sections, necessary to study very fine-grained calcite aggregates under the optical microscope, is not required. (2) For well-etched surfaces in the absence of twin boundaries, the automatic generation of grain boundary maps can be up to 2–3 times faster and is less subjective than manual tracings. (3) The identification of different minerals is easy because of the changes in topographic relief and the use of EDS. Furthermore, capturing of BSE images or elemental maps allow segmentation of the different minerals and the automatic quantification of both rock composition and microstructural parameters. The generation of these parameters using optical microscopy, in contrast, would be tedious and extremely time consuming.

Cheaper equipment and preparation costs (i.e. time argument) represent the major advantages of the two-step etching method compared to the more sophisticated orientation contrast or EBSD approaches. Furthermore, only one third of an image acquired with these two approaches has been measured. The other two thirds are artificially reconstructed by simply stretching the image because of the required specimen tilting. This procedure is not necessary for the etching method.

Although the paper focuses on automatic grain boundary detection, the etched surfaces also provide an excellent basis for manual grain boundary tracings even if the aggregates consist of many twinned calcite grains.

3. Part II: Grain size analysis of a calcite dolomite mylonite

In part II, the two-step etching technique is applied to study the microstructural changes in a carbonate mylonite as a function of changing calcite–dolomite content. Although recent microstructure research has focused increasingly on polyphase material (e.g. Handy, 1990; Bruhn et al., 1999), little attention has been paid to low temperature deformation microstructures of calcite dolomite mixtures, probably because of their extremely fine grain size. As will be shown below, two-step etching is a way out of this dilemma.

The sample investigated derives from the basal thrust of the Doldenhorn nappe and was deformed at

about 340°C (Burkhard, 1990). The specimen is characterised by an intercalation of dolomite and calcite bands whose thicknesses vary from a few microns up to a few millimetres. To estimate the influence of changing dolomite calcite content on the grain size of recrystallised calcite grains, four areas of a carbonate mylonite with variable calcite dolomite modal composition (calcite 30–98%) were analysed (Fig. 4). According to the technique outlined in the previous sections, element distribution maps were acquired and grain boundary maps of the calcite grains were generated. The modal compositions (Table 2) and the grain size variations of the calcite grains (Fig. 4) were obtained by using processed elemental maps and calcite grain boundary outlines, respectively.

Besides the major constituents calcite and dolomite, only minor amounts of mica, quartz, apatite and hematite are present (Table 2). In the calcite-dominated (Cc-98) and the dolomite-dominated (Cc-30) end members, the minor phase typically appears in the form of isolated grains (Fig. 4). Additionally, Cc-30 calcite grains are clustered in aggregates of elongate shape. The long axes of the bigger aggregates are subparallel to the shear plane while the long axes of smaller calcite lenses are obliquely oriented. Within areas of intermediate composition to calcite dominated zones (Cc-48 and Cc-88) the calcitic phase is always

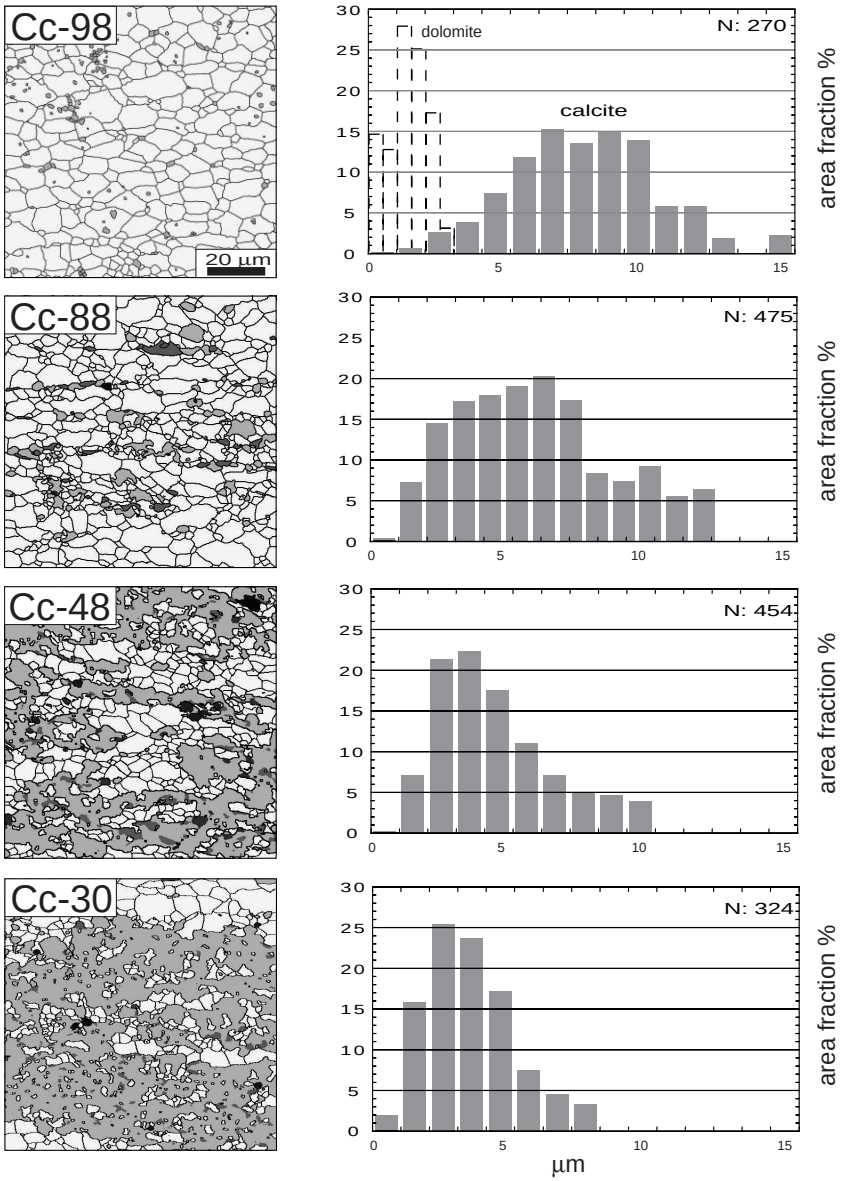

Fig. 4. Calcite mylonite with variable dolomite content. First column: microstructures showing the calcite (white) grain boundaries and distribution of dolomite (bright grey) and accessories (dark grey) of quartz, mica, apatite and hematite. Second column: grain size histograms show area fraction vs. grain size interval. Note that the grain sizes represent equivalent radii.

Table 2
Modal compositions and wt% of minerals within the analysed microstructures

Label	Ratio cc/dol	Calcite area %	wt%	Dolomite area %	wt%	Mica area %	wt%	Quartz area %	wt%	Apatite area %	wt%	Hematite area %	wt%
Cc-98	49/1	**98.0**	**97.9**	**2.0**	**2.1**	–	–	–	–	–	–	–	–
Cc-88	10/1	**88.5**	**89.0**	**8.9**	**9.4**	2.5	1.5	–	–	0.1	0.1	–	–
Cc-48	1.1/1	**48.1**	**47.6**	**44.6**	**46.5**	4.7	2.8	1.1	1.0	0.9	1.0	0.6	1.0
Cc-30	1/2.2	**30.0**	**29.3**	**67.0**	**68.9**	2.9	1.7	–	–	0.1	0.1	–	–

interconnected and surrounds dolomite cores. This interconnectivity results from cycles of brittle fracturing of the dolomite aggregates and calcite precipitation in the fractures. Note that calcite in these fractures is completely overprinted by dynamic recrystallisation.

Examination of individual calcite grains reveals that most major axes are slightly oblique with respect to the foliation (Fig. 4). In terms of grain boundary geometries, calcite–calcite grain boundaries are straight to slightly curved but calcite–dolomite phase boundaries often show a lobate character (Fig. 4).

Both the mean value and the range of the calcite grain size distribution decrease as a function of increasing dolomite content (second column in Figs. 4 and 5). Unfortunately, the two-step etching treatment does not attack the dolomite grain boundaries, precluding the quantification of grain size distribution in dolomite aggregates. However, grain sizes of individual dolomite grains in Cc-98 (Fig. 4, uppermost row) and in recrystallised rims of dolomite porphyroclasts (Fig. 6) imply a small average grain size (1.5–2 μm) for the recrystallised dolomite, which seems to be invariant with changing modal composition.

The observed trend of decreasing grain size with increasing dolomite content could be caused several factors: (a) increasing grain boundary pinning in calcite grains by the dolomite (e.g. Olgaard and Evans, 1988), (b) a switch in deformation mechanism from dislocation creep in the calcite rich parts to diffusion creep in the calcite dolomite mixtures (see for example Olgaard, 1990; Bruhn et al., 1999) and (c) stress concentration in calcite as a mechanically weak phase around the more rigid dolomite aggregates (compare for example with fig. 6 in Handy, 1990). To determine

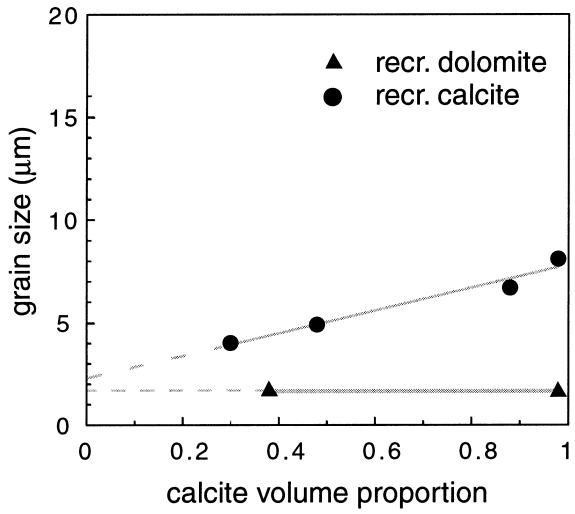

Fig. 5. Mean values of equivalent radii of recrystallised calcite and dolomite grains as a function of the rock modal composition. The dolomite grain size at 37% calcite derives from the recrystallised dolomite grains in Fig. 6.

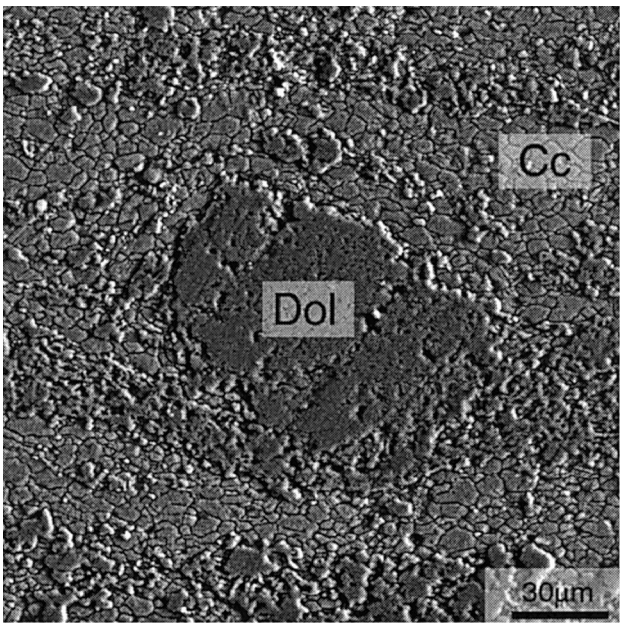

Fig. 6. Dolomite–calcite mixtures. Rotated dolomite clast of region B with a dynamically recrystallised rim (BSE image). Cc: calcite, Dol: dolomite.

which of these fractures is operating requires further investigations (TEM, EBSD). The combination of two-step etching and TEM in future studies will provide insight into the deformational behaviour of fine-grained carbonates.

4. Conclusions

Two-step etching with weak hydrochloric and acetic acids has proved to be a useful technique for the visualisation of microstructures of fine-grained carbonate mylonites. The procedure permits automatic generation of grain boundary maps, allowing further calculation of the microstructural parameters with image analysis software. Although the etching technique presented above can only be applied to calcite aggregates, the combination of surface etching and digital image analysis may be an interesting approach in microstructural analysis of all fine-grained materials (e.g. dolomite, olivine quartz, feldspars). For these minerals, however, new etching techniques have to be designed and tested. In conjunction with these tests, careful checks must be performed to determine whether etching really reflects microstructural elements like grain and subgrain boundaries or simply artefacts.

Acknowledgements

Susan Ellis kindly improved the English. Karsten Kunze is gratefully acknowledged for acquiring the orientation contrast image and for reviewing an earlier version of the manuscript. The two journal referees Pat Trimby and an anonymous reviewer helped significantly to improve this article.

References

Adams, B.L., Wright, S.I., Kunze, K., 1993. Orientation imaging: The emergence of a new microscopy. Metallurgical Transactions 24A, 819–831.

Burkhard, M., 1990. Ductile deformation mechanisms in micritic limestones naturally deformed at low temperatures (150–350°C). In: Knipe, R.J., Rutter, E.H. (Eds.), Deformation Mechanisms, Rheology and Tectonics, Geological Society Special Publication 54, pp. 241–257.

Burkhard, M., 1993. Calcite twins, their geometry, appearance and significance as stress–strain markers and indicators of tectonic regime: a review. Journal of Structural Geology 15, 351–369.

Bruhn, D.F., Olgaard, D.L., Dell'Angelo, L.N., 1999. Evidence for enhanced deformation in two-phase rocks: Experiments on the rheology of calcite anhydrite aggregates. Journal of Geophysical Research 104, 701–724.

Casey, M., Kunze, K., Olgaard, D.L., 1998. Texture of Solnhofen limestone deformed to high strains in torsion. Journal of Structural Geology 20, 255–267.

Dietrich, D., Song, H., 1984. Calcite fabrics in natural shear environment, the Helvetic nappes of western Switzerland. Journal of Structural Geology 6, 19–32.

Dunlap, W.J., Hirth, G., Teyssier, C., 1997. Thermomechanical evolution of a ductile duplex. Tectonics 16, 983–1000.

Exner, H.E., 1972. Analysis of grain- and particle-size distributions in metallic materials. International Metallurgical Review 17, 25–42.

Goldstein, J.L., Newbury, D.E., Echlin, P., Joy, D.C., Romig, A.D., Lyman, C.E., Fiori, C., Lifshin, E., 1992. Scanning Electron Microscopy and X-Ray Microanalysis, 2nd ed. Plenum Press, New York.

Handy, M.R., 1990. The solid-state flow of polymineralic rocks. Journal of Geophysical Research 95, 8647–8661.

Heilbronner, R., 2000. Automatic grain boundary detection and 3-D grain size analysis of dynamically recrystallized quartzite. Journal of Structural Geology (in press).

Heilbronner, R., Bruhn, D., 1998. The influence of three-dimensional grain size distributions on the rheology of polyphase rocks. Journal of Structural Geology 20, 695–707.

Herwegh, M., Handy, M.R., 1998. The origin of shape preferred orientations in mylonite: inferences from in-situ experiments on polycrystalline norcamphor. Journal of Structural Geology 20, 681–694.

Olgaard, D.L., Evans, B., 1988. Grain growth in synthetic marbles with added mica and water. Contributions to Mineralogy and Petrology 100, 246–260.

Olgaard, D.L., 1990. The role of second phase in localizing deformation. In: Knipe, R.J., Rutter, E.H. (Eds.), Deformation Mechanisms, Rheology and Tectonics, Geological Society Special Publication 54, pp. 241–257.

Panozzo Heilbronner, R., 1992. The autocorrelation function: an image processing tool for fabric analysis. Journal of Structural Geology 12, 351–370.

Panozzo, R., 1983. Two-dimensional analysis of shape-fabric using projections of digitized lines in a plane. Tectonophysics 95, 279–294.

Panozzo, R., 1984. Two-dimensional strain from the orientation of lines in a plane. Journal of Structural Geology 6, 215–221.

Pauli, Ch., Schmid, S.M., Heilbronner, R., 1996. Fabric domains in quartz mylonites: localized three-dimensional analysis of microstructure and texture. Journal of Structural Geology 18, 1183–1203.

Pfiffner, A.O., 1982. Deformation mechanisms and flow regimes in limestone from the Helvetic zone of the Swiss Alps. Journal of Structural Geology 4, 429–442.

Prior, D.J., Trimby, P.W., Weber, U.D., Dingley, D.J., 1996. Orientation contrast imaging of microstructures in rocks using forescatter detectors in the scanning electron microscope. Mineralogical Magazine 60, 859–869.

Rutter, E.H., 1998. Use of extension testing to investigate the influence of finite strain on the rheological behavior of marble. Journal of Structural Geology 20, 243–254.

Schmid, S.M., Panozzo, R., Bauer, S., 1987. Simple shear experiments on calcite rocks: rheology and microfabric. Journal of Structural Geology 9, 747–778.

Schmid, S.M., Paterson, M.S., Boland, J.N., 1977. Superplastic flow in fine-grained limestone. Tectonophysics 43, 257–291.

Schmid, S.M., Paterson, M.S., Boland, J.N., 1980. High temperature flow and dynamic recrystallization in Carrara marble. Tectonophysics 65, 245–280.

Trimby, P., Prior, D., 1999. Microstructural imaging techniques: A comparison between light and scanning electron microscopy. Tectonophysics 303, 71–81.

Van Der Pluijm, B.A., 1991. Marble mylonites in the Bancroft shear zone, Ontario, Canada: microstructures and deformation mechanisms. Journal of Structural Geology 13, 1125–1135.

Walker, A.N., Rutter, E.H., Brodie, K.H., 1990. Experimental study of grain-size sensitive flow of synthetic, hot pressed calcite rocks. In: Knipe, R.J., Rutter, E.H. (Eds.), Deformation Mechanisms, Rheology and Tectonics, Geological Society Special Publication 54, pp. 241–257.

Wegner, M.W., Christie, J.M., 1983. Chemical etching of deformation sub-structures in quartz. Physics and Chemistry of Minerals 9, 67–78.